5.2

CYCLONE TRACKS IN THE VICINITY OF GREENLAND – ASPECTS OF AN INTERACTION PROCESS

Cornelia B. Schwierz* and Huw C. Davies
Institute for Atmospheric and Climate Science, ETH Zürich, Switzerland

1. INTRODUCTION

Greenland (GL) is the third-largest orographic feature on the Northern Hemisphere and is located contiguous to the North Atlantic storm track. Both factors imply that it has the potential to exert a significant impact upon planetary- and synoptic-scale flow.

The ambient flow response to a topographic obstacle is influenced by the scale, geometry and location of the orography as well as the strength and structure of the incident air stream. In essence, GL falls into the quasi-geostrophic, but nonlinear part of parameter space.

Here primary focus is on the interaction of synoptic-scale vorticity features with an orographic obstacle of GL-scale and location, and the approach is that of a numerical-cum-diagnostical study. The aim is to elicit the quintessential dynamical features of the interaction that can ensue in realized events.

The paper is structured as follows: First the numerical model and diagnostical tools are introduced (Section 2). Thereafter (Section 3) a rudimentary climatology of cyclone tracks in the GL area is presented. The derived climatology prompt a series of questions related to the splitting of the storm-tracks by GL, and these questions are then addressed in a series of short studies. In Section 4 the dominant synoptic-scale local flow structures at a mountain of GL-scale and location are described. The interaction of a cyclone advecting toward GL is studied in Section 5 and theoretical considerations are invoked to interpret the nature of the balanced flow perturbation. Section 6 summarises the results.

2. METHODOLOGY

2.1 Data and Cyclone Tracking

The diagnostic part of the study is performed using the ECMWF 15-yr Re-analysis data set (ERA15; Gibson et al. 1997) with a horizontal resolution of 1°. The tracking of cyclones is undertaken with the standard sea level pressure data, and minima are detected as closed isolines with a resolution of 2 hPa. The tracking itself is performed on a 6-hourly basis applying a nearest neighbour search.

2.2 Model and Basic Flow State

The nature of the flow response to GL-scale orography is investigated using numerical simulations performed with an adiabatic version of the primitive equation forecast model (EM) of the German Weather Service (Majewski 1991). This model is operated on a sphere with GL as the only topographic feature present within an idealised zonal wind field. Ambient settings examined include a barotropic westerly flow of (a) uniform angular velocity, i. e. the spherical equivalent of a constant zonal field on an f-plane; (b) uniform potential vorticity and (c) an additional localized vortex advecting toward the mountain. Here we present results of (a) and (c).

*Corresponding author address: Institute for Atmospheric and Climate Science, Swiss Federal Institute of Technology, Hönggerberg HPP, 8093 Zürich, Switzerland, e-mail: schwierz@atmos.umnw.ethz.ch

3. OBSERVED CYCLONE TRACKS

Evolving extra-tropical low-pressure systems typically travel along preferred paths that have historically been discerned by inspection of weather charts (Petterssen 1956) or more recently with numerical tracking routines (Hoskins and Hodges 2002). Figure 1 shows the 15-yr total of winter (DJF) cyclone tracks in the North Atlantic as detected by our analysis.

The distribution of cyclone paths is not unlike the 850 hPa vorticity track density field of Hoskins and Hodges (2002). The main cyclone paths are clearly evident. Typically a cyclone forms off New Foundland and are traverses in a north-easterly direction towards GL. There the tracks split into two main branches, straddling its coasts. The easterly branch continues into the Norwegian Sea, whereas the westerly branch is directed first northward and then curves anticyclonically around the poleward edge of GL. Another source region for systems approaching GL is over Hudson Bay. It is also interesting to note (not shown), that for different large-scale circulation regimes (e. g. opposite phases of the NAO), the anticyclonic portion of the westerly branch is affected much less, whereas the easterly branch is much more coherent and contains more members for stronger westerlies (positive phases of the NAO).

4. AMBIENT FLOW RESPONSE

To analyse in more detail the dynamic processes involved in the interaction of cyclones with high orography, we pursue a two-stage modelling approach. First the local flow response is examined of an idealised superrotational westerly flow field impinging on GL.

For the quasi-steady state (Fig. 2) the isentropic streamlines correspond to air parcel trajectories. In accord with the occurrence of weak flow upstream, the parcel tracks respond to the large-scale obstacle, decelerate and deviate from their zonal path. The air is first deflected northwards ahead of the mountain and then back south to almost its original latitude in the lee of the mountain. In doing so it undergoes major latitudinal excursions of $\pm 2000\,\mathrm{km}$ and air of very different origin and history can merge in the wake.

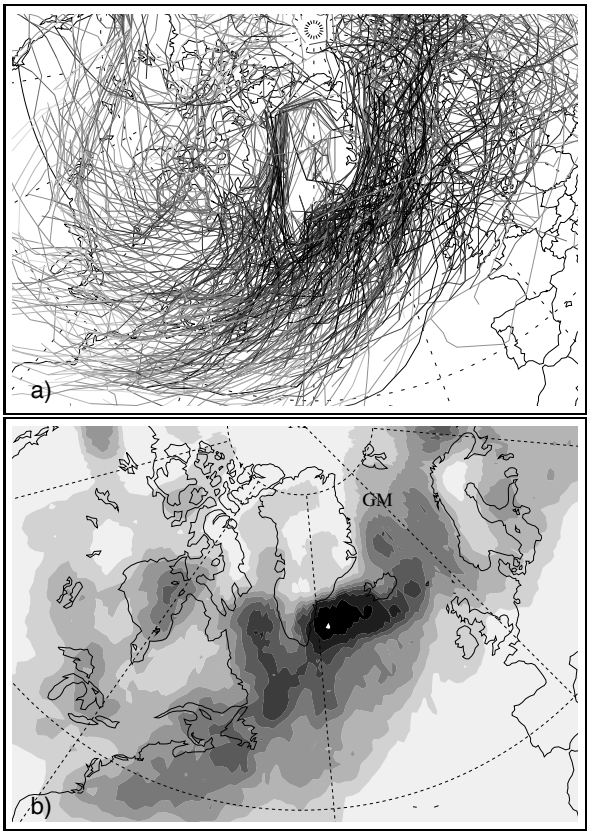

Figure 1: 15-year winter (DJF) cyclone tracks in the North Atlantic. a) individual tracks (shading indicates intensity, lower pressure values darker); b) density of the tracks.

At lower levels (285 K, Fig. 2a), the flow splits around the terrain. Upstream blocking and the downstream wake cover a distance of about $\sim$1000 km. Stagnation is associated with flow splitting and is also found in the wake region. Rotational effects can shift the stagnation point to the south of an obstacle (Schär and Davies 1988). Here the splitting line is located at the far southern tip of GL, whereas at higher levels just above mountain crest (295 K, Fig. 2b) the dominant feature is the mountain anticyclone aloft, generated by vortex shrinking. A stagnant region with closed streamlines forms and is reminiscent of a Taylor Cap (Huppert 1975).

The velocity distribution displays some characteristics that are familiar from synoptic analysis fields (e. g. Doyle and Shapiro, 1999). (i) Enhanced flow along the northern slope, the maximum being slightly on the downwind side; (ii) a pronounced jet at GL's southern tip with a maximum perturbation velocity (decaying upwards) and (iii) a nearly stagnant wake region (with contemporaneous recirculation) just north of the tip jet, resulting in an area of high meridional velocity gradients, i. e. the co-located vorticity maximum is mainly due to shear vorticity. Curvature vorticity is largest at the northern and southern tips, in conjunction with the deformation field (not shown).

The essence of the aforementioned features is well-reproduced with idealised elliptic mountain experiments (not shown). Results obtained with elliptical obstacles on the f-/β-plane (Peng et al. 1995, Ólafsson and Bougeault 1996, Doyle and Shapiro 1999) have stressed the N-S-asymmetry that occurs as a result of rotation. Here, it is interesting to note, that the proximity to the pole on the spherical domain adds to the asymmetry. While obstacles on a plane or in midlatitudes produce almost symmetrical bands of positive (negative) vorticity to the south (north), positive vorticity to the north is related to the curvature of the flow and weakens the band of negative vorticity.

The observed vorticity and flow field distributions have ramifications for studying cyclone tracks in the region. This aspect will be addressed further in the following Section. For realised events in nature, there are many other factors that come into play. For GL low-level inversions are crucial for cold-air outbreaks and downslope windstorms, and both can affect cyclone tracks and evolution in that region.

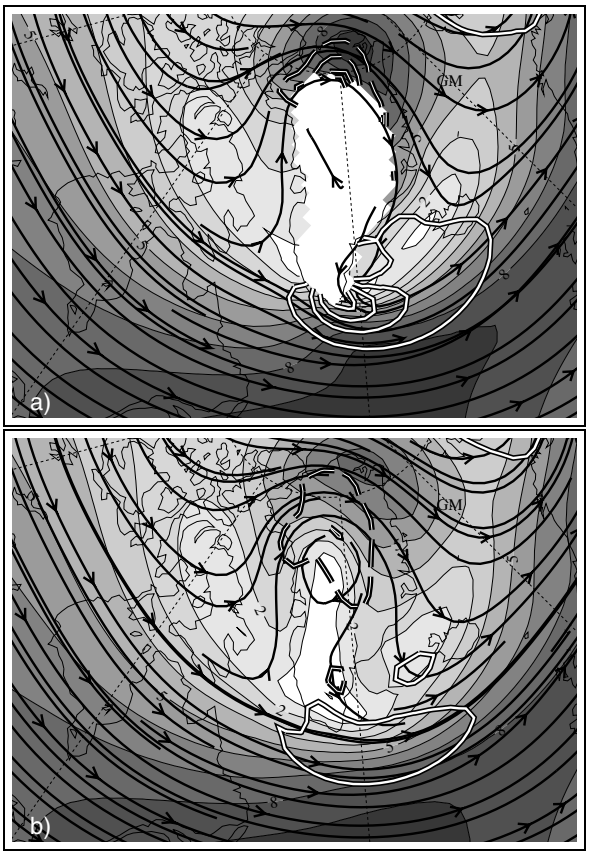

Figure 2: Idealised flow response to GL topography. Velocity (shaded, contour interval 1 m/s), isentropic streamline pattern and vorticity (white contours, interval 0.1/s) on levels a) 285 K and b) 295 K.

5. CYCLONE-MOUNTAIN INTERACTION

Here consideration is given to a cyclonic vortex advecting towards the mountain to analyse the interaction. The basic physical setting comprises a purely barotropic zonal flow of uniform vertical stratification and potential vorticity, a compact and vertically coherent balanced vortex that is set on track to intercept an elliptical-shaped topographic feature of GL-scale and location (Fig. 3a). See Schwierz and Davies (2002) for further details of the experiment.

The vortex is associated with a circumferential velocity of $\sim$15 ms^{-1} in the lower troposphere and has a per-

turbation surface pressure signature of ~ -48 hPa compared to the zonal basic state. In line with these features the vortex carries a distinct signal in its near-surface potential temperature field of ~ 10 K.

The strength of the ambient flow and the dimensions of the topography are associated with values of $\mathcal{R}o \sim 0.1 - 0.5$ and $\mathcal{F}^{-1} \sim 2 - 3$, hence the incident flow can surmount the terrain, and the dominant component of the flow is a balanced orographically-induced anticyclone astride the topography with an almost isentropic underlying surface. The orographic-anticyclone is associated with circumferential velocities ($\sim 20\,\mathrm{ms}^{-1}$) that are comparable to that of the vortex.

5.1 Evolution of Eulerian Features

The evolution of the surface vortex anomaly divides into three overlapping phases. In a first phase ($t \lesssim 150$ h) the vortex pattern retains its compact character although it is embedded in an ambient flow of non-constant angular velocity, and the vortex advects eastward with the mean flow whilst contemporaneously experiencing a weak retardation and mild poleward drift. In a second phase (t$\sim$ 150-240 h) the vortex approaches and deflects anticyclonically around the topography whilst concurrently appearing to lose much of its spatial coherency. In the third phase ($t \gtrsim 240$ h) the severely disrupted vortex recovers much of its axisymmetric structure on the lee-side. Thereafter the partially reconstituted but reduced in amplitude vortex is advected downstream away from the topography.

A notable feature of all three phases is that the orographic-anticyclone is comparatively unperturbed throughout although it is approached by a vortex whose velocity signal is of comparable strength.

Information on the non-linear nature of the interaction can be gained by examining the evolution of the meridional flow component in the vicinity of the orography during the second and third phases (not shown). The accompanying low-level horizontal deformation field in the vicinity of the topography is $\sim 1.0 \cdot 10^{-4}\,\mathrm{s}^{-1}$ prior to the arrival of the vortex, and would in isolation suffice to severely distort a passive scalar advecting past the terrain within the ambient flow (see later). The approach of the vortex increases the strength of the deformation field by a factor of ~ 5 first on the windward side and later in the northern lee region.

5.2 Lagrangian Features

The foregoing description is supported by examining the Lagrangian evolution of the ensemble of selected air parcels using the combined trajectory and diagnosis routine of Wernli and Davies (1997). It is applied to the output of the numerical PE simulation accessed with a 2 h temporal resolution.

The *first* trajectory ensemble (Figs. 4a) is indicative of the nature of the orographic modification of the flow prior to the approach of the vortex. It corresponds to 150 h forward trajectories from an elliptical region initially located at 850 hPa upstream of the orography at t=0 h. In addition the temporal evolution of vorticity and deformation along these trajectories is visualised. These quasi-passive trajectories experience minor deformation (factor 3-4) due to the ambient mountain-induced flow perturbation (cf. Section 4). The envelope of the ensemble is established by the combination of (i) the passive advection, (ii) the moderate shear deformation and (iii) the unperturbed ambient flow.

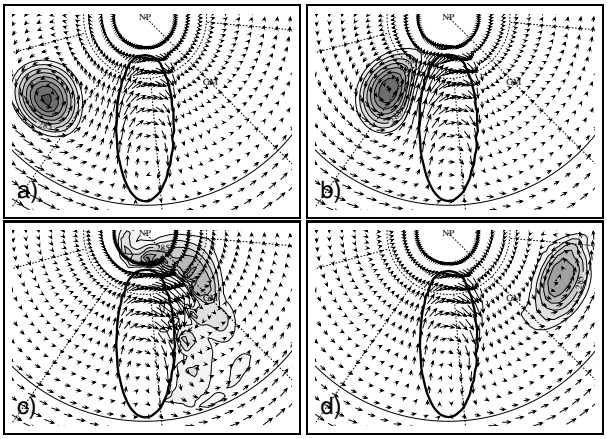

Figure 3: Time sequence (a) 150 h, b) 180 h, c) 240 h, d) 330 h) of surface potential temperature and wind. Orography indicated by bold line.

The *second* ensemble (Figs. 4b) is a set of 150 h forward trajectories of air parcels initially located at 850 hPa within the core of the vortex at t=150 h. Note that these parcels emanate from the same geographical location as those of the first ensemble. The trajectories are consistent with vortex-elongation on the windward side and recompaction to the lee. The air parcels within the vortex first retain their cyclonic rotation in the approach to the mountain and are then severely distorted to a filamentary form during the phase of poleward circumnavigation (i. e. at 70-80 h trajectory time). It is pertinent to note that the polar location of the mountain implies an enhanced curvature of the flow, and hence additional strain upon the air parcels. The shear process sets in on the windward side and reaches its maximum slightly downwind of the mountain's axis of symmetry. Note that an air parcel rotating within the vortex experiences a differential deformation field: much stronger deformation while in close proximity to the mountain, in comparison to the far-side of the vortex. This is consistent with the non-linear velocity increase due to the mountain anticyclone interaction. The envelope of the air parcels recovers its original shape in the lee, and a small portion of trajectories split from the main body.

The contrast in the envelope of the two ensembles (Fig. 4) points to the strength and role of the non-linear interaction between the vortex and the orographic-induced flow. This influences the location, timing and extent of vortex reconstitution.

5.3 Discussion

The foregoing sequence of events is interpreted in terms of the combined influence of the orographic-anticyclone and the self-dynamics of the vortex. Both are essentially balanced flow systems, and a simple phenomenological account of the flow evolution can be proffered from a quasi-geostrophic PV perspective.

The vortex's poleward drift during this phase can then be linked to the far-field influence of the orographic-anticyclone, whereas its simulated weak zonal retardation must be accounted for by the latitudinal gradient of the ambient flow's angular velocity.

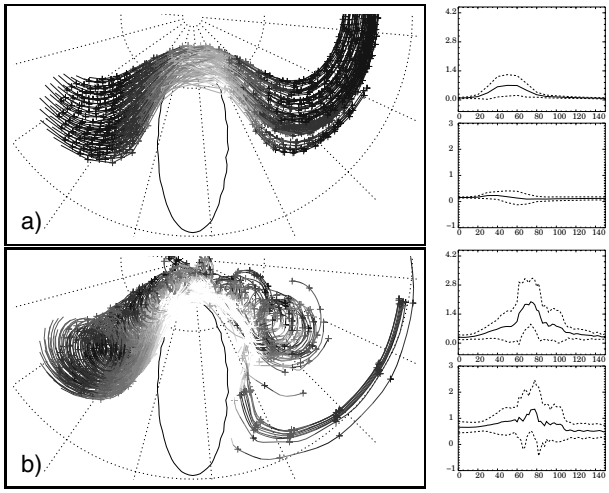

Figure 4: 150 h-forward trajectories started on 850 hPa (a) within the "free" atmosphere at t=0 h (shading: deformation, large values: white). b) Analogue to a) but started from within the surface vortex anomaly at t=150 h. Right column: time evolution of mean and standard deviation for each selected trajectory ensemble of deformation (a,b upper rows) and vorticity (a,b lower rows).

The second phase is characterized by an acceleration of the vortex's poleward drift, and its rapid distortion to form a filament that arches around the topography. Both effects are consistent with the changes in the vortex's ambient field as it approaches the topography, since that change comprises an increase in the ambient circumferential velocity and provides a surface deformation field.

In the third phase the newly-formed filament's continued circumnavigation of the topography is consistent with its advection within the anticyclone's circumferential velocity field. In contrast its reconstitution to form a compact vortex is at variance with the influence of the anticyclone's deformation field acting alone upon the vortex. This conundrum is resolved by recognizing the coupled effect of the filament's self-induced motion and the influence of the ambient deformation field. In isolation the elongated filament would tend to rotate cyclonically such that its leading edge moves further away from the terrain and its trailing edge approaches closer. In effect the realization of this rotation allows the ambient deformation field to recompact the vortex. The present flow development is an extension of the tumbling vortex dynamics (Meacham et al. 1990) illustrating the partial dissolution and subsequent reconstitution of a PV vortex within a highly spatially- and temporally-varying deformation field.

Finally consider the robustness of the orographic-anticyclone throughout the flow evolution. This is linked to the anticyclone's dependence upon the PV of the incident airstream, but not on its amplitude and direction. Thus the structure and amplitude of the orographic anticyclone remains unmodified by the approach of the vortex until, or rather unless, a portion of the incident vortex's anomalous potential vorticity or surface potential temperature ascends onto the topography. From a climatological standpoint it is pertinent to note that the January monthly-mean field of vorticity on the 700 hPa surface does show a predilection for negative anomalies - the possible vestige of orographically-bound anticyclones - to occur over significant mountain ranges (cf. Hsu, 1987).

6. FINAL REMARKS

Inspite of their high idealisation the foregoing experiments illustrate some of the fundamental aspects that govern cyclone tracks in the vicinity of large-scale topography. For Greenland with its particular scale and polar location, the underlying dynamics can be interpreted using quasi-geostrophic theory, and are a combination of ambient low-level flow features and non-linear vortex-vortex-interaction. These findings are consistent with observed paths of low-pressure systems in the Baffin Bay region.

Acknowledgments: The authors are indebted to H. Wernli for kindly making the cyclone track data available.

References

Doyle, J. D., and M. A. Shapiro. 1999. Flow response to large-scale topography: the Greenland tip jet. *Tellus A* **51**, 728–748.

Gibson, J. K., A. Hernandez, P. Kållberg, A. Nomura, E. Serrano, and S. Uppala. 1997. ERA description. *ECMWF Re-Analysis Project Report Series 1*. ECMWF, Reading, UK.

Hoskins, B. J., and K. I. Hodges. 2002. New Perspectives on Northern Hemisphere Winter Storm Tracks. *J. Atmos. Sci.* **59**, 1041–1061.

Hsu, H.-H. 1987. Propagation of low-level circulation features in the vicinity of mountain ranges. *Mon. Wea. Rev.* **115**, 1864–1892.

Huppert, H. E. 1975. Some remarks on the initiation of inertial Taylor columns. *J. of Fluid Mech.* **67**, 397–412.

Majewski, D. 1991. The Europa-Modell of the Deutscher Wetterdienst. *Numerical methods in atmospheric models*. Vol. 2. ECMWF, Reading, UK.

Meacham, S. P., G. R. Flierl, and U. Send. 1990. Vortices in shear. *Dyn. Atmos. Oceans* **14**, 333–386.

Ólafsson, H., and P. Bougeault. 1996. Nonlinear flow past an elliptic mountain ridge. *J. Atmos. Sci.* **53**, 2465–2489.

Peng, M. S., S. W. Li, S. W. Chang, and R. T. Williams. 1995. Flow over mountains - Coriolis-force, transient troughs and 3 dimensionality. *Quart. J. Roy. Meteor. Soc.* **121**, 593–613.

Petterssen, S. 1956. *Weather Analysis and Forecasting*. In: Motion and motion systems. Pp. 428. Vol. I. McGraw-Hill.

Schär, C., and H. C. Davies. 1988. Quasi-geostrophic stratified flow over isolated finite amplitude topography. *Dynamics of Atmospheres and Oceans* **11**, 287–306.

Schwierz, C., and H. C. Davies. 2002. Evolution of a synoptic-scale vortex advecting toward a high mountain. *Tellus*. accepted.

Wernli, H., and H. C. Davies. 1997. A Lagrangian-based analysis of extratropical cyclones. Part I: The method and some applications. *Quart. J. Roy. Meteor. Soc.* **123**, 467–489.